*Supplementary Information*

# DNA scaffolds support stable and uniform peptide nanopores

*Evan Spruijt, Samuel E. Tusk, Hagan Bayley*

# Supplementary Methods

### *Coarse-grained molecular dynamics simulations (oxDNA2)*

All coarse-grained molecular dynamics simulations were performed by using the oxDNA2 simulation code, available from http://dna.physics.ox.ac.uk[1,2]. We used a periodic cubic box of 150 units (128 nm). To generate the input configurations, the single-stranded oligos were hybridized using temporary harmonic traps between complementary bases. The resulting configuration was used as input in a constraint-free virtual-move Monte Carlo simulation with a total of 2 x $10^7$ steps, until the free energy no longer decreased. End configurations of that simulation were used as input in subsequent molecular dynamics simulations with and without constraints. All simulations were performed at 25ºC and at an ionic strength of 0.5 M.

To probe the flexibility of the scaffold, an external force was applied to all terminal 3′ and 5′ nucleotides in the direction perpendicular to the plane of the ring. To maintain a zero net force, the same external force was applied in the opposite direction to all hinge nucleotides (Supplementary Data 1 and Fig. 1a). Alternatively, a radial force was applied to push all arms outward, implemented as sets of harmonic traps between terminal 5′ nucleotides of every pair of arms at opposite ring positions with an equilibrium separation of 19.5 nm. The applied forces were increased linearly from 0 to their final value during a 1.5 µs loading stage and kept constant afterwards.

Configurations were visualised using VMD[3] and Chimera (UCSF)[4]. An atomic model of the scaffold was made from coarse-grained configurations by using a Python script kindly provided by Dr Lorenzo Rovigatti[5]. The base order, which is 3′→ 5′ in the oxDNA files, was inverted using a custom-written Matlab script to comply with the 5′→ 3′ PDB convention, and missing P-O bonds were added using the PyMol bond tool.

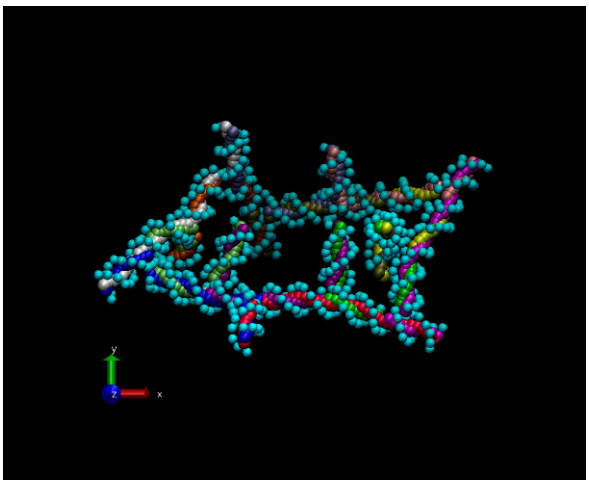

**Movie S1**. OxDNA2 coarse-grained MD simulation of the DNA scaffold without external force applied to the arms. Duration: 0.152 ms, framerate: 16.4 µs$^{-1}$.

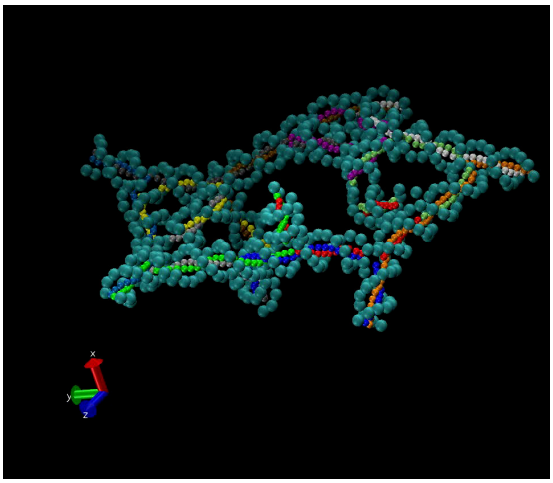

**Movie S2**. OxDNA2 coarse-grained MD simulation of the DNA scaffold with an external force applied to all terminal 3′ and 5′ nucleotides in the direction perpendicular to the plane of the ring leading to a down-pointing orientation of all arms within 5 µs. Duration: 30 µs, framerate: 11.6 µs$^{-1}$.

## *Transmission electron microscopy*

Samples for TEM were annealed at a strand concentration of 100 nM in 100 mM Tris.HCl buffer, pH 7.5, without added salt. The annealed mixture was 50-100 times diluted in 100 mM Tris.HCl buffer, applied to freshly glow-discharged 400-mesh carbon-coated copper grids (TAAB) and stained with 2 mM uranyl acetate. EM images were made with a Fei Tecnai 12 Transmission Electron Microscope equipped with a 4 Megapixel Gatan Ultrascan 1000 CCD camera.

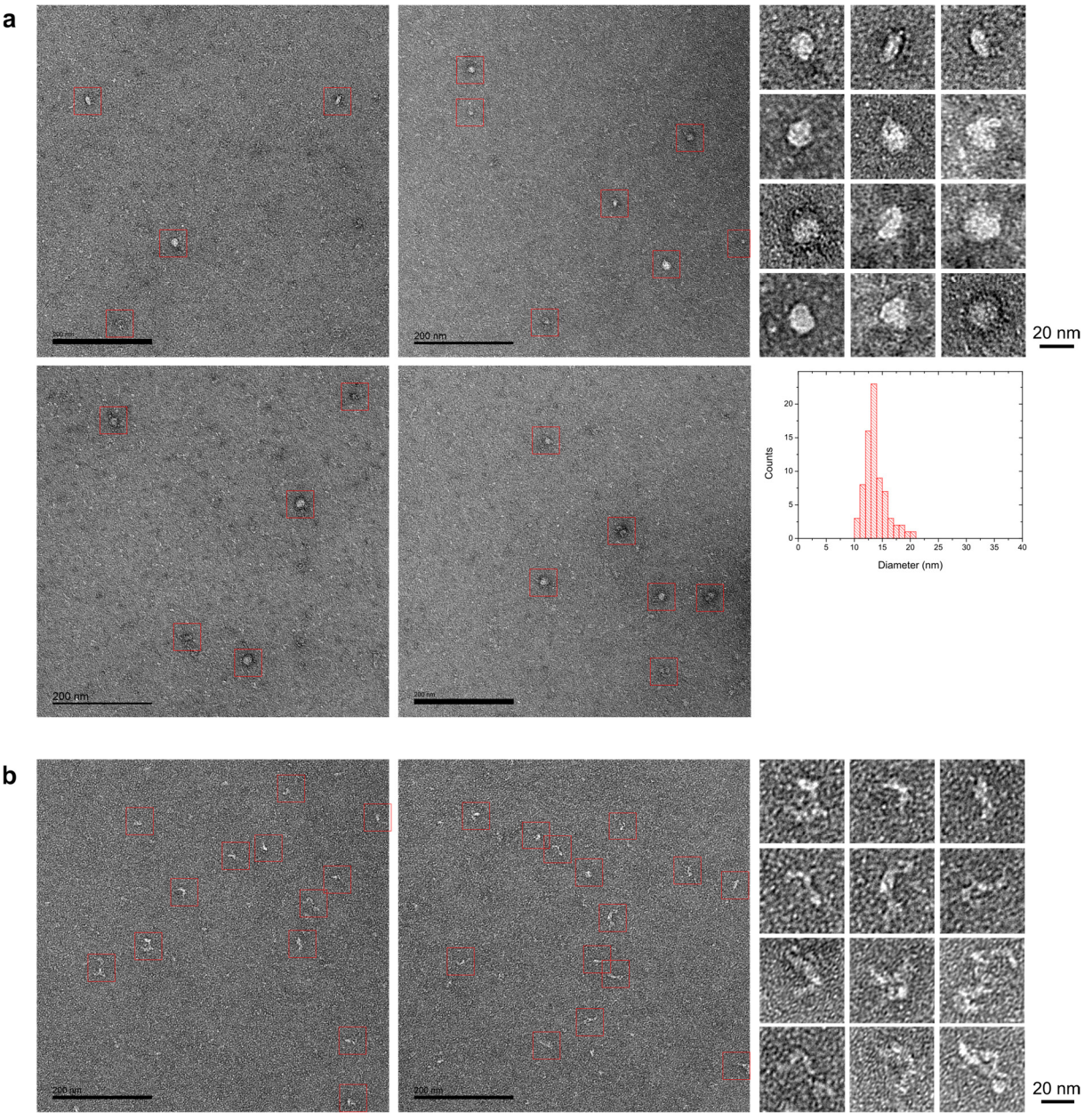


**Figure S1. a**, TEM images of DNA scaffold rings (see Figure 1b for an acrylamide gel analysis), a composite of single rings (top right), and a histogram of ring diameters (bottom right). Scale bars: left and middle 200 nm, right 20 nm. The diameter of the rings is 13.8 ± 2.0 nm (expected: 13.0 nm). **b**, TEM images of *RsaI* digested DNA scaffold rings (see Figure 1e for an acrylamide gel analysis), and a composite of individual structures. Scale bars: left and middle 200 nm, right 20 nm. The contour length of the individual digested rings is 44 ± 6 nm (expected: 41 nm).

### *Mass spectrometry of intact DNA scaffolds*

DNA rings for native mass spectrometry were annealed by mixing 12 oligonucleotides in equal amounts at a strand concentration of 500 nM in 10 aliquots of 100 µL in 100 mM NH4Ac, pH 7.5 and 0.5 M NaCl. The aliquots were combined and purified by five subsequent filter and dilution steps with 1 M ammonium acetate pH 7.5 in Amicon Ultra spin filters with a cutoff molecular weight of 100,000 Da. After the last dilution the DNA rings were concentrated in the same spin filters to final scaffold concentration of 14 µM. Spectra were acquired on a Synapt1 mass spectrometer (Waters) modified for high masses[6,7] using gold-coated glass capillaries prepared in-house[8]. Optimized instrument parameters were as follows: capillary voltage 1.8 kV, cone voltage 200 V, extractor 5 V, source backing pressure 7–10 mbar, and a collision cell pressure of 10 psi. Collision cell energy was 30–80 V. Spectra were processed and assigned using MassLynx software.

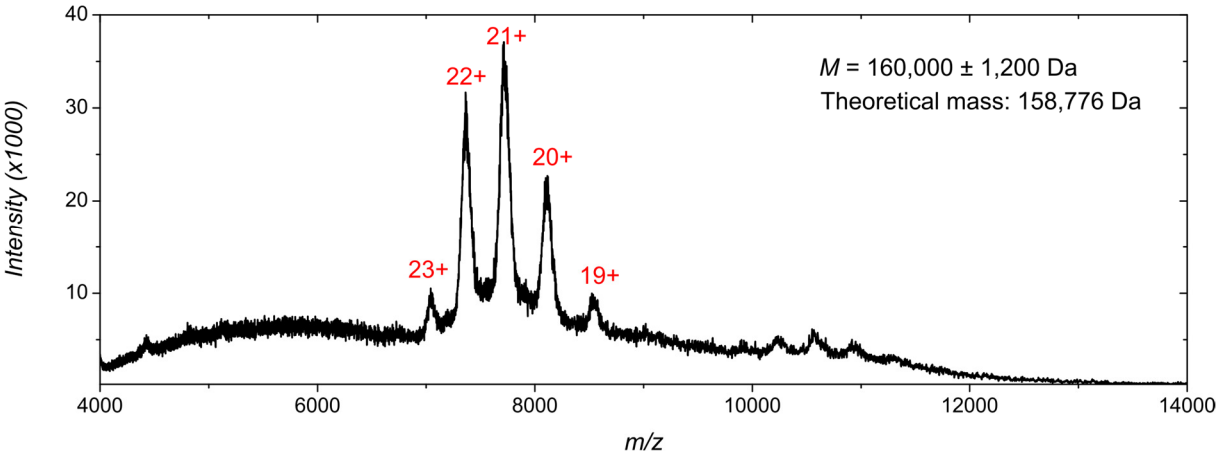


**Figure S2.** Native mass spectrometry of DNA scaffold rings. The theoretical mass is calculated as the sum of the theoretical masses of the twelve individual oligos without 5′ amino-C6 group (see Supplementary Data 1 for the sequences).

### *Stepwise photobleaching*

Alexa-647 labeled oligos were prepared by incubating 1 nmol of each 5′ amino-C6 modified oligo in 100 mM potassium phosphate, pH 7.2, with 50 nmol of Alexa-647 NHS ester (50 mg/mL in DMSO) in a total volume of 20 µL at room temperature for 2 h. Labeled oligos were purified by HPLC (Agilent Infinity 1260 series) on a $C_{18}$ column (4.6 x 150 mm) by using 10 mM tetraethylammonium bromide (TEAB) in MilliQ water, pH 8.5, as the binding buffer (A), and in acetonitrile for elution (B). Labeled oligos were eluted by using a shallow gradient of 5% to 35% B over 30 min at 1 mL/min, as monitored by the absorbance at 260 and 636 nm. The Alexa-modified fractions were lyophilized, dissolved in 20 µL 100 mM potassium phosphate, pH 7.2, and diluted to 500 nM. The purity of the labeled oligos was checked by HPLC and from the ratio of the absorbance at 260 and 647 nm (see Table S1 for details).

The purified Alexa-647 labeled oligos were assembled into ring-shaped scaffolds for use in stepwise photobleaching experiments following the same procedure as for unlabeled oligos. A biotin group, attached to the 3′ end of one of the Alexa-647 labeled oligos, was used

to anchor the rings to streptavidin-modified glass slides. Control samples with no biotinylated oligos were prepared to check for nonspecific adsorption to the glass slides. For annealing, twelve Alexa-647 labeled oligos or twelve Alexa-647 labeled oligos, of which one contained a 3′ biotin, were mixed in equal amounts at a strand concentration of 40 nM in a total volume of 30 µL, containing 100 mM Tris.HCl, pH 7.5 and 0.5 M NaCl. The oligos were then annealed in a Veriti Thermal Cycler (Applied Biosystems) by heating the sample for 3 min at 95ºC, cooling to 65ºC in 3 min and finally cooling to 4ºC in 4 h. The samples were used immediately after annealing.

Single-molecule photobleaching steps were counted with total internal reflection fluorescence (TIRF) microscopy, using excitation at 633 nm. DNA scaffolds with single biotin anchors were diluted to 0.5 pM in degassed TBSG (100 mM Tris.HCl pH 7.5, 0.5 M NaCl and 0.8% (w/v) D-glucose). These scaffolds were immobilized on streptavidin-modified glass slides that prepared as described elsewhere[9], after checking for nonspecific adsorption of a 0.5 pM solution of non-biotinylated scaffolds, and imaged in the presence of an oxygen radical scavenging system[10,11]. Images were corrected for drift and single-molecule fluorescence intensities were obtained from circular Gaussian fits to the spots. Full photobleaching traces shorter than 3 second and steps that deviated by more than 50% from the average photobleaching step size were excluded from the analysis.

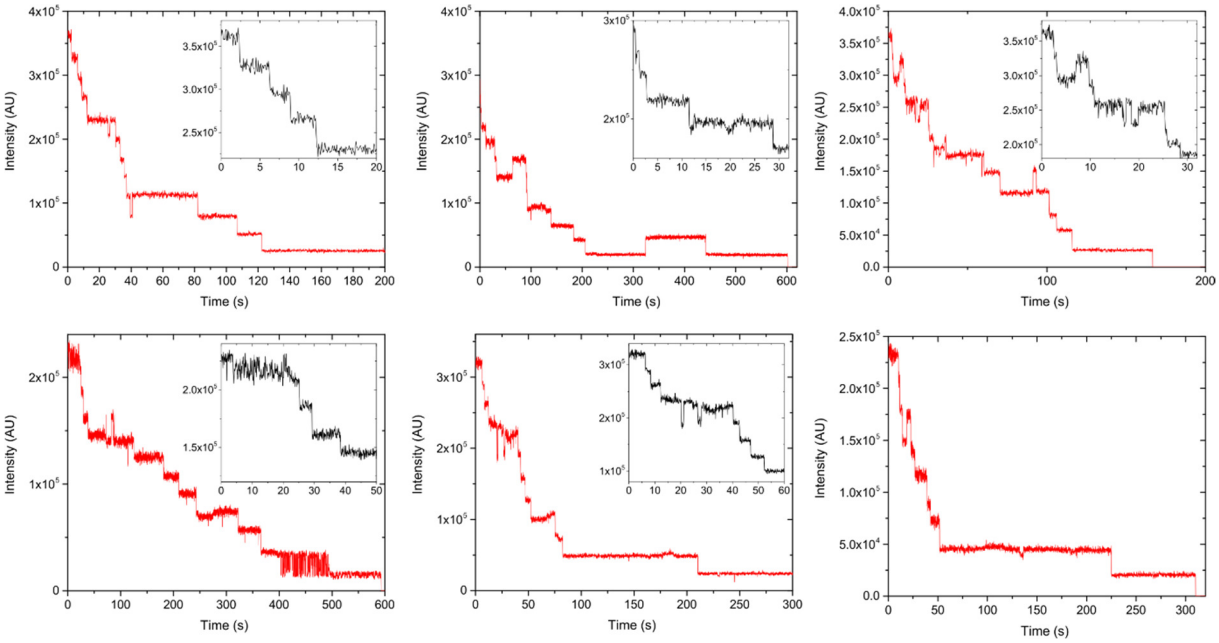


**Figure S3**. Additional traces of the stepwise photobleaching of a single DNA scaffolds with 12 Alexa-647-modified oligos, attached to the surface via a single biotin-streptavidin bond. Insets show a zoomed-in view of the initial part of the traces.

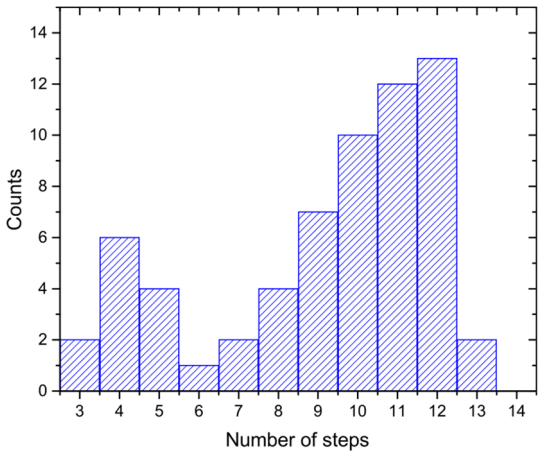


**Figure S4**. Distribution of the number of photobleaching steps for DNA scaffolded with 12 Alexa-647-modified oligos.

## *Synthesis and purification of oligo-tagged PEG-5k probes*

Oligonucleotide-tagged PEG-5k probes were prepared as follows. Amino-C3 modified 11c′ (8-mer) or 11d′ (19-mer, see Supplementary Data 1) (100 nmol) was reacted with 500 nmol dibenzocyclooctyne-sulfo-*N*-hydroxysuccinimidyl ester in 250 µL 100 mM potassium phosphate, pH 7.2. Without purification, the product was reacted with 10 µmol PEG-5k-azide (100 mg/mL) in 100 mM potassium phosphate, pH 7.2. The adduct was purified by electrophoresis in a 10% acrylamide gel. The PEG-5k modified oligo was extracted from the appropriate gel band, subjected to buffer exchange and then concentrated by using Amicon 3k spin filters. The final oligo concentration was determined from the absorbance at 260 nm.

# Supplementary Data 1: DNA sequences

## *Basic ring-shaped scaffold*

The oligonucleotide sequences of this design are as follows.

```
 (1) 5′ [AmC6]-GCCTCGAATCACTCCACTGAACCATCCTCTTGATCTTGTGAAC 3′
 (2) 5′ [AmC6]-TGCCATAAGTATTCAGTGGAGCAGCAACATAGACTCTCAACAA 3′
 (3) 5′ [AmC6]-GTTCACAAGAATCGAAACCAATGTTAGTGTAGAGTGCATAAGC 3′
 (4) 5′ [AmC6]-CCAACTGGGAATTGGTTTCGACAAGAGGATGGAACTTATGGCA 3′
 (5) 5′ [AmC6]-GCTTATGCACAGAGTCACAGAACGGGAAGCAGAAACGTGTGAG 3′
 (6) 5′ [AmC6]-TCGAGCAATAATCTGTGACTCCTACACTAACAATCCCAGTTGG 3′
 (7) 5′ [AmC6]-CTCACACGTTAGATACGGACACTTGGATAGCGAAAAGCACCTC 3′
 (8) 5′ [AmC6]-CACTTCACTTATGTCCGTATCCTGCTTCCCGTATATTGCTCGA 3′
 (9) 5′ [AmC6]-GAGGTGCTTTATGTCAATCGGAGTAGCCTAGCAAGCCTTAGCC 3′
(10) 5′ [AmC6]-GAAACAGATAACCGATTGACACGCTATCCAAGAAAGTGAAGTG 3′
(11) 5′ [AmC6]-GGCTAAGGCTAAATGAGTACCCTATGTTGCTGAGATTCGAGGC 3′
(12) 5′ [AmC6]-TTGTTGAGAGAGGTACTCATTGCTAGGCTACTATATCTGTTTC 3′
```

All oligos used for conjugation were modified with a 5′ amino-C6 group. All oligos contain two adenosine hinge bases (at positions 11 and 33) included to increase the flexibility of the arms. The oligo sequences were optimized to give low melting temperatures for all non-complementary strands and high melting temperatures for (partially) complementary strands, as shown below.

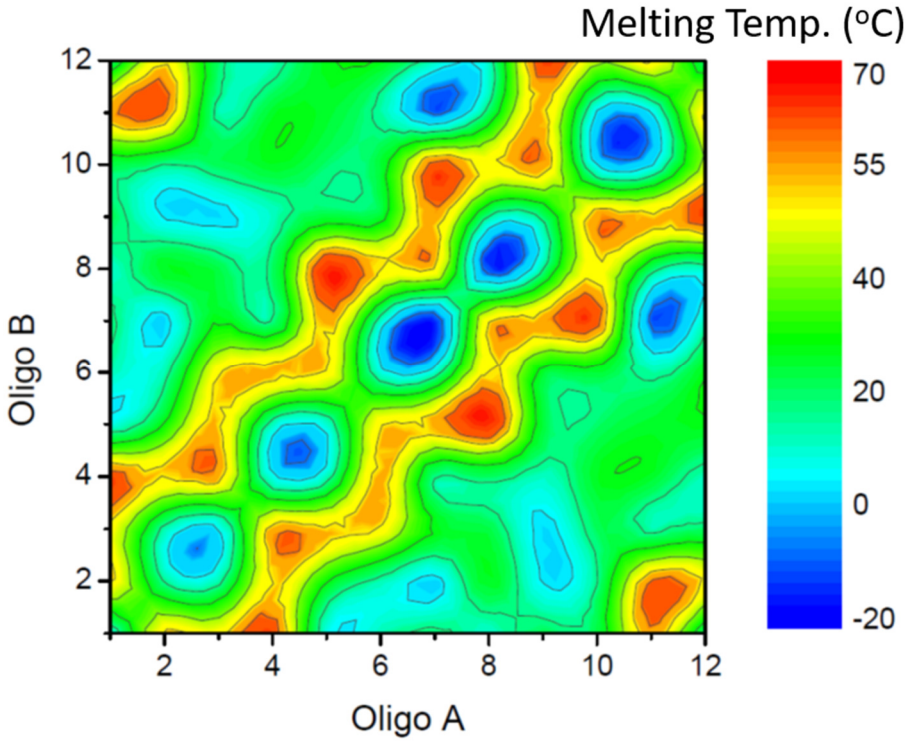


**Figure S5.** 2D melting diagram of oligonucleotide duplexes, predicted using the DinaMelt webserver.

### *Opened rings*

The opened rings used in the restriction assay in Fig. 1e were prepared from strands 1-10 of the basic ring, complemented with 11a/b and 12a/b below. These constructs are designed to be identical to the restriction product of the closed ring (oligos 1-12) with *RsaI* and were used as a control in Fig. 1e.

```
(11a) 5′ GGCTAAGGCTAAATGAGT                 3′
(11b) 5′ ACCCTATGTTGCTGAGATTCGAGGC          3′
(12a) 5′ TTGTTGAGAGAGGT                     3′
(12b) 5′ ACTCATTGCTAGGCTACTATATCTGTTTC      3′
```

### *Rings with docking site*

Rings with docking sites used in the experiments in Fig. 4 were prepared from strands 1-10 and 12 of the basic ring, complemented with an elongated oligo-11c (8-mer) or oligo 11d (19-mer):

```
(11c) 5′ GGCTAAGGCTAAATGAGTACCCTATGTTGCTGAGATTCGAGGCACTTACTGAGC            3′
(11d) 5′ GGCTAAGGCTAAATGAGTACCCTATGTTGCTGAGATTCGAGGCACTTACTGAGCACTATCTGAGC 3′
```

The tags and tagged oligos used for binding to the docking sites are:

```
(11c′)      5′ [AmC3]-GCTCAGTA                    3′
(11d′)      5′ [AmC3]-GCTCAGATAGTGCTCAGTA         3′
(11d′c30)   5′ C30ATCCCATCCCGCTCAGATAGTGCTCAGTA   3′
(11d-toe)   5′ TACTGAGCACTATCTGAGCGGGATGGGATGGG   3′
```

### *Rings with biotin handles*

Rings with one or two biotin handles for stepwise photobleaching experiments were prepared from 5′ Alexa-647 labelled strands 1,2,4-9,11 and 12 of the basic ring, and 5′-Alexa-647, 3′-biotin modified strands 3 and 9. The biotinylated strands were synthesized from:

```
(3Bio) 5′ [AmC6]-GTTCACAAGAATCGAAACCAATGTTAGTGTAGAGTGCATAAGC-[Bio] 3′
(9Bio) 5′ [AmC6]-GAGGTGCTTTATGTCAATCGGAGTAGCCTAGCAAGCCTTAGCC-[Bio] 3′
```

# Supplementary Data 2: Peptide sequences

The peptide sequences used in this work are (cysteines used for conjugation to the DNA are highlighted in red):

```
CGG-cWza[T376R]       : NH2- CGGAPLVRWNRVISQLVPTITGVHDLTETVRYIKRWPN    -COOH
    cWza-GGC[T376R]   : NH2-    APLVRWNRVISQLVPTITGVHDLTETVRYIKRWPNGGC -COOH
(E.coli) Wza-D4-R376T: NH2-    APLVRWNRVISQLVPTISGVHDMTETVRYIKTWPN    -COOH
```

All peptides were purchased from Peptide Protein Research Ltd (Fareham, UK), as HPLC-purified (>95%) lyophilized powders. The molecular masses were verified by MALDI mass spectrometry and the peptides were used without further purification.

# Supplementary Data 3: Purification of peptide-oligo conjugates

**Table S1**. Characterization of peptide-oligo conjugates and Alexa-labeled oligos.

| Name | Length | Concentration | Mass theor. | Mass exper. | Delta Mass | Yield | Purity |
|---|---|---|---|---|---|---|---|
| | (nt) | (ng/uL) | (g/mol) | (g/mol) | (ppm) | (%) | (%) |
| 1-PEG2-Mal-CWza | 43 | 806 | 17870.4 | 17871.4 | 58 | 15.5 | 98.6 |
| 2-PEG2-Mal-CWza | 43 | 924 | 18049.2 | 18048.2 | -53 | 17.5 | 99.7 |
| 3-PEG2-Mal-CWza | 43 | 1048 | 18144.2 | 18144.3 | 7 | 19.7 | 99.2 |
| 4-PEG2-Mal-CWza | 43 | 1150 | 18192.2 | 18192.0 | -9 | 21.5 | 99.3 |
| 5-PEG2-Mal-CWza | 43 | 1095 | 18220.2 | 18220.8 | 35 | 20.5 | 99.6 |
| 6-PEG2-Mal-CWza | 43 | 1031 | 17967.2 | 17966.3 | -48 | 19.6 | 99.6 |
| 7-PEG2-Mal-CWza | 43 | 340 | 18026.2 | 18026.5 | 19 | 6.4 | 100 |
| 8-PEG2-Mal-CWza | 43 | 1336 | 17858.2 | 17858.9 | 41 | 25.6 | 99.6 |
| 9-PEG2-Mal-CWza | 43 | 1113 | 18095.2 | 18095.3 | 7 | 21.0 | 99.5 |
| 10-PEG2-Mal-CWza | 43 | 1039 | 18147.2 | 18146.8 | -20 | 19.5 | 100 |
| 11-PEG2-Mal-CWza | 43 | 1143 | 18159.2 | 18159.7 | 29 | 21.4 | 99.4 |
| 12-PEG2-Mal-CWza | 43 | 1270 | 18081.2 | 18081.3 | 7 | 24.0 | 99.7 |

| Name | Length | Concentration | Mass theor. | Mass exper. | Delta Mass | Yield | Purity |
|---|---|---|---|---|---|---|---|
| | (nt) | (ng/uL) | (g/mol) | (g/mol) | (ppm) | (%) | (%) |
| 1-PEG2-Mal-WzaC | 43 | 792.6 | 17870.4 | 17871.6 | 69 | 30.4 | 98.7 |
| 2-PEG2-Mal-WzaC | 43 | 515.2 | 18049.2 | 18049.1 | -4 | 19.5 | 96.6 |
| 3-PEG2-Mal-WzaC | 43 | 480.8 | 18144.2 | 18144.3 | 7 | 18.1 | 98.0 |
| 4-PEG2-Mal-WzaC | 43 | 431.8 | 18192.2 | 18191.9 | -15 | 16.2 | 97.6 |
| 5-PEG2-Mal-WzaC | 43 | 473.1 | 18220.2 | 18219.8 | -20 | 17.7 | 98.8 |
| 6-PEG2-Mal-WzaC | 43 | 518.8 | 17967.2 | 17968.3 | 63 | 19.8 | 98.5 |
| 7-PEG2-Mal-WzaC | 43 | 486.6 | 18026.2 | 18026.6 | 24 | 18.4 | 97.9 |
| 8-PEG2-Mal-WzaC | 43 | 397.8 | 17858.2 | 17858.4 | 13 | 15.3 | 97.0 |
| 9-PEG2-Mal-WzaC | 43 | 278.1 | 18095.2 | 18096.2 | 57 | 10.5 | 98.0 |
| 10-PEG2-Mal-WzaC | 43 | 433.1 | 18147.2 | 18147.6 | 24 | 16.3 | 97.9 |
| 11-PEG2-Mal-WzaC | 43 | 396.8 | 18159.2 | 18158.3 | -48 | 14.9 | 97.9 |
| 12-PEG2-Mal-WzaC | 43 | 468.2 | 18081.2 | 18080.2 | -53 | 17.7 | 98.9 |

| Name | Length | Concentration | Mass theor. | Mass exper. | Delta Mass | Yield | Purity |
|---|---|---|---|---|---|---|---|
| | (nt) | (ng/uL) | (g/mol) | (g/mol) | (ppm) | (%) | (%) |
| 1-PEG4-SS-CWza | 43 | 273.8 | 17893.5 | 17894.6 | 62 | 21.0 | 96.4 |
| 2-PEG4-SS-CWza | 43 | 361.9 | 18072.3 | 18072.6 | 17 | 27.4 | 94.0 |
| 3-PEG4-SS-CWza | 43 | 357.9 | 18167.3 | 18165.9 | -77 | 26.9 | 96.0 |
| 4-PEG4-SS-CWza | 43 | 261.6 | 18215.3 | 18213.6 | -93 | 19.6 | 94.5 |
| 5-PEG4-SS-CWza | 43 | 295.9 | 18243.3 | 18245.0 | 93 | 22.1 | 96.7 |
| 6-PEG4-SS-CWza | 43 | 340.7 | 17990.3 | 17990.9 | 34 | 25.9 | 92.7 |
| 7-PEG4-SS-CWza | 43 | 277.5 | 18049.3 | 18049.5 | 11 | 21.0 | 95.6 |
| 8-PEG4-SS-CWza | 43 | 376 | 17881.3 | 17883.3 | 112 | 28.9 | 95.5 |
| 9-PEG4-SS-CWza | 43 | 299 | 18118.3 | 18118.2 | -5 | 22.6 | 95.6 |
| 10-PEG4-SS-CWza | 43 | 352.8 | 18170.3 | 18169.9 | -22 | 26.5 | 92.9 |
| 11-PEG4-SS-CWza | 43 | 386 | 18182.3 | 18183.3 | 55 | 29.0 | 96.5 |
| 12-PEG4-SS-CWza | 43 | 146.3 | 18104.3 | 18102.5 | -99 | 5.5 | 97.3 |

| Name | Length | A260 | Conc. DNA | Conc. DNA | A647 | Conc. Alexa647 | Labeling eff. |
|---|---|---|---|---|---|---|---|
| | (nt) | (-) | (ng/µL) | (µM) | (-) | (µM) | (%) |
| 1-[5'-Alexa647] | 43 | 1.265 | 42.2 | 3.24 | 0.856 | 3.17 | 98 |
| 2-[5'-Alexa647] | 43 | 0.709 | 23.6 | 1.79 | 0.427 | 1.58 | 88 |
| 3-[5'-Alexa647] | 43 | 0.244 | 8.1 | 0.61 | 0.156 | 0.58 | 95 |
| 3-[5'-Alexa647][3'-Biotin] | 43 | 0.376 | 12.5 | 0.94 | 0.242 | 0.90 | 95 |
| 4-[5'-Alexa647] | 43 | 0.500 | 16.7 | 1.25 | 0.382 | 1.41 | 113 |
| 5-[5'-Alexa647] | 43 | 0.359 | 12.0 | 0.89 | 0.254 | 0.94 | 105 |
| 6-[5'-Alexa647] | 43 | 0.616 | 20.5 | 1.56 | 0.427 | 1.58 | 101 |
| 7-[5'-Alexa647] | 43 | 0.715 | 23.8 | 1.81 | 0.480 | 1.78 | 98 |
| 8-[5'-Alexa647] | 43 | 0.950 | 31.7 | 2.43 | 0.644 | 2.39 | 98 |
| 9-[5'-Alexa647] | 43 | 0.468 | 15.6 | 1.18 | 0.308 | 1.14 | 97 |
| 9-[5'-Alexa647][3'-Biotin] | 43 | 0.457 | 15.2 | 1.15 | 0.368 | 1.36 | 119 |
| 10-[5'-Alexa647] | 43 | 0.906 | 30.2 | 2.27 | 0.593 | 2.20 | 97 |
| 11-[5'-Alexa647] | 43 | 0.734 | 24.5 | 1.84 | 0.504 | 1.87 | 102 |
| 12-[5'-Alexa647] | 43 | 0.333 | 11.1 | 0.84 | 0.211 | 0.78 | 93 |

# Supplementary Data 4: Electrical recordings

## *Structural details of Wza peptide-bearing DNA scaffolds*

**Table S2**. Configurational details and experimental information of DNA scaffolds bearing Wza peptides used in electrical recordings. The number of Wza peptides was varied from 1 to 12.

| # peptides per scaffold | Arms* | # experiments | # pores | Conductance ** (nS) | Outliers *** (nS) |
|---|---|---|---|---|---|
| 1 | 1 | | | | |
| 2 | 1,7 | 3 | 0 | | |
| 3 | 2,6,10 | 2 | 0 | | |
| 4 | 1,4,7,10 (2,5,8,11) | 5 | 0 | | |
| 5 | 2,4,6,9,11 (1,3,5,8,10) | 6 | 1 | | 0.46 |
| 6 | 1,3,5,7,9,11 (2,4,6,8,10,12) | 23 | 4 | | 0.53, 0.52, 0.53, 0.49 |
| 7 | 1,3,4,5,7,9,11 (2,4,6,8,10,11,12) | 13 | 2 | | 1.28, 1.27 |
| 8 | 2,3,5,6,8,9,11,12 | 163 | 124 | 1.46 ± 0.06 | |
| 9 | 1,2,3,5,6,7,9,10,11 | 11 | 8 | 1.46 ± 0.07 | 1.71, 1.84 |
| 10 | 1-5,7-11 | 28 | 19 | 1.47 ± 0.06 | 1.96 |
| 11 | 1-11 | 14 | 8 | 1.50 ± 0.05 | |
| 12 | 1-12 | 27 | 21 | 1.48 ± 0.07 | |

* In most experiments the modified arms were selected to be as much as possible radially symmetric and the numbers in this column indicate the typical choice of modified arm numbers (alternative configurations in brackets). Control experiments with more asymmetric distributions of modified arms were carried out as well for the scaffolds with 8 peptides (arms 1-8 and arms 1-4,7-10), but we did not observe any differences in the conductance or rectification of the current compared to the scaffolds with symmetrically distributed arms.

** Only stable pores (> 1 min) are included in the averages. Both conjugates with fixed and cleavable scaffolds are included in the averages.

*** Individual nanopores are counted as outliers when the measured conductance is more than 3σ separated from the average conductance value for the octamers.

## *Naked DNA scaffold*

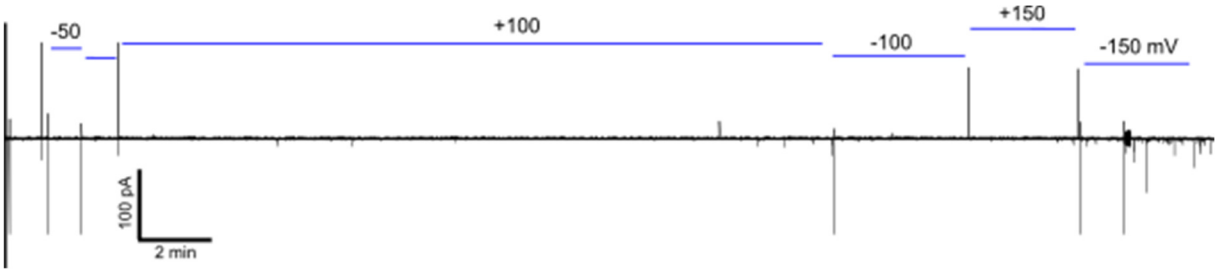


**Figure S6**. Electrical recording of naked DNA scaffold at 100 nM. The applied potential is indicated at the top of the trace.

## *Free Wza peptides*

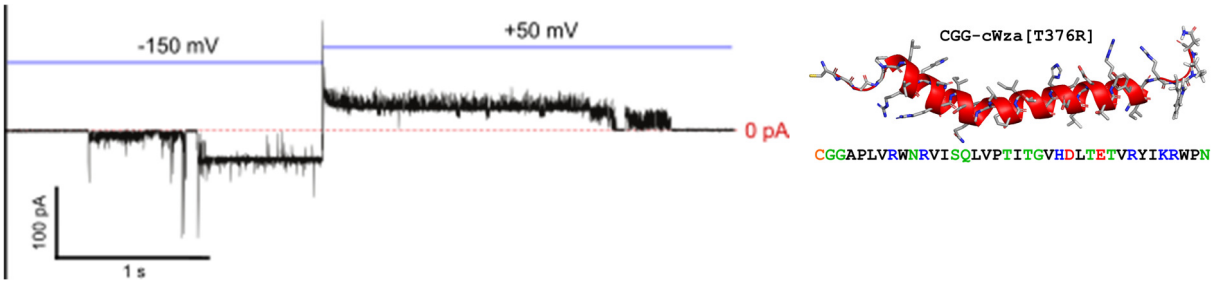


**Figure S7**. Electrical recording of events elicited by free CGG-cWza[T376R] peptides (250 nM). The applied potential is indicated at the top of the trace. The I-V profile of these events resembles that of the L state of scaffolded Wza nanopores (Fig. S12), but their mean lifetime is of the order of seconds (Fig. S13), whereas scaffolded Wza nanopores are stable for at least an hour (Fig. S6). A transition to a higher conductance state has not been observed for these unscaffolded peptides.

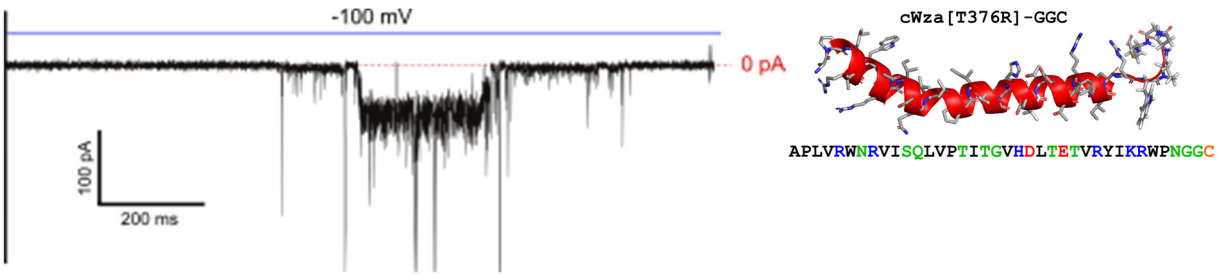


**Figure S8**. Electrical recording of events elicited by free cWza[T376R]-GGC peptides (400 nM). The applied potential is indicated at the top of the trace. The mean conductance of these events is smaller than either the L- or H-state of scaffolded Wza nanopores, and their mean lifetime is shorter than a second at any applied potential.

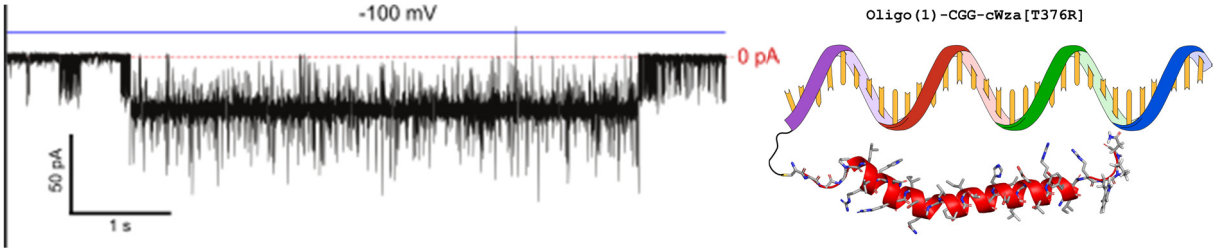


**Figure S9**. Electrical recording of events elicited by free oligo1-Wza conjugates (400 nM). The applied potential is indicated at the top of the trace. The I-V profile of these events resembles that of the L state of scaffolded Wza nanopores (Fig. S12), but their mean lifetime is of the order of seconds (Fig. S13), whereas scaffolded Wza nanopores are stable for at least an hour (Fig. S6). A transition to a higher conductance state has not been observed for these unscaffolded peptides.

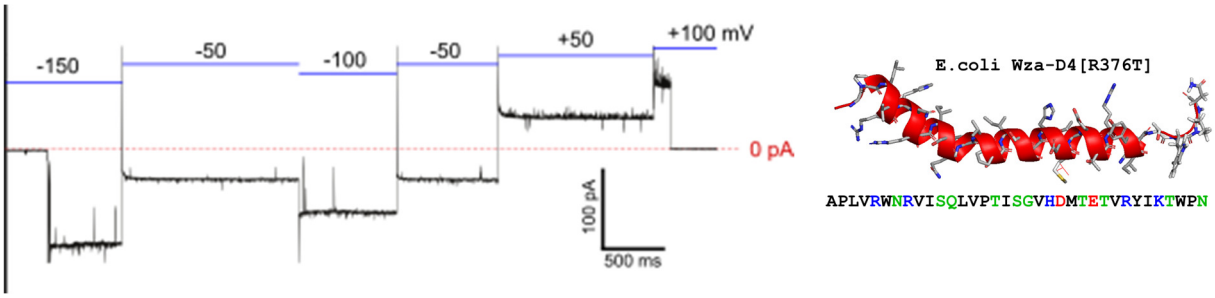


**Figure S10**. Electrical recording of events elicited by free *E.coli* Wza D4[R376T] peptides (250 nM). The applied potential is indicated at the top of the trace. These peptides differ from the Wza peptides used for scaffolding: they have only one cationic residue near the C-terminus instead of two, which seems to enhance their stability. The I-V profile of these events is shown in Fig. S12 and resembles that of the L-state of scaffolded Wza nanopores at negative applied potentials. Their mean lifetime at positive applied potentials is of the order of seconds, whereas scaffolded Wza nanopores are stable for at least an hour (Fig. S6). A transition to a higher conductance state has not been observed for these unscaffolded peptides.

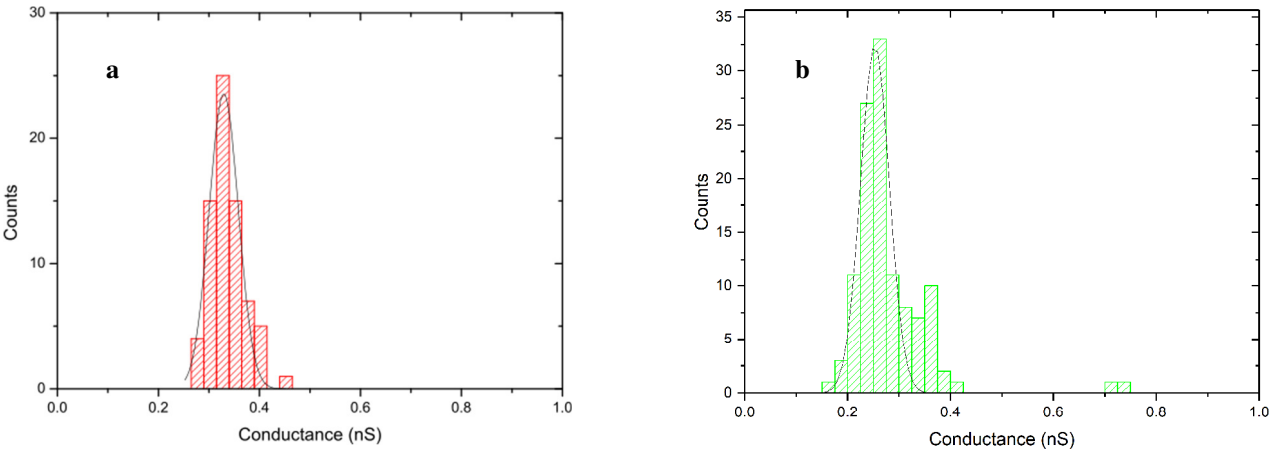


**Figure S11**. Event histograms of the mean conductance of events elicited by (a) free CGG-cWza[T376R] peptides at +50 mV (72 events in 3 experiments) and (b) oligo(1)-Wza conjugates at -50 mV (118 events in 2 experiments).

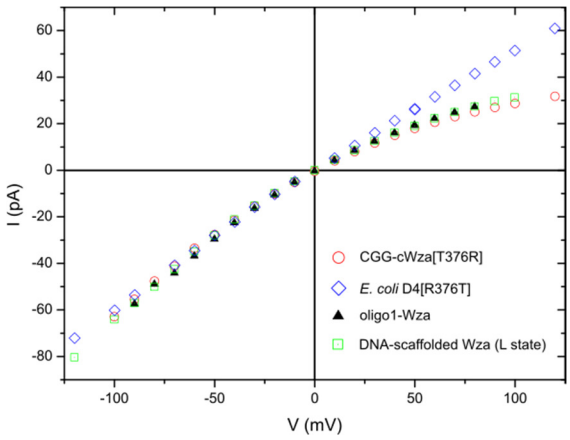


**Figure S12**. I-V profiles of nanopores formed from free peptides, free oligo-Wza conjugates and the intermediate L-state of DNA-scaffolded Wza peptides. Characteristic I-V curves of both the L and H-state are shown in Fig. 3f.

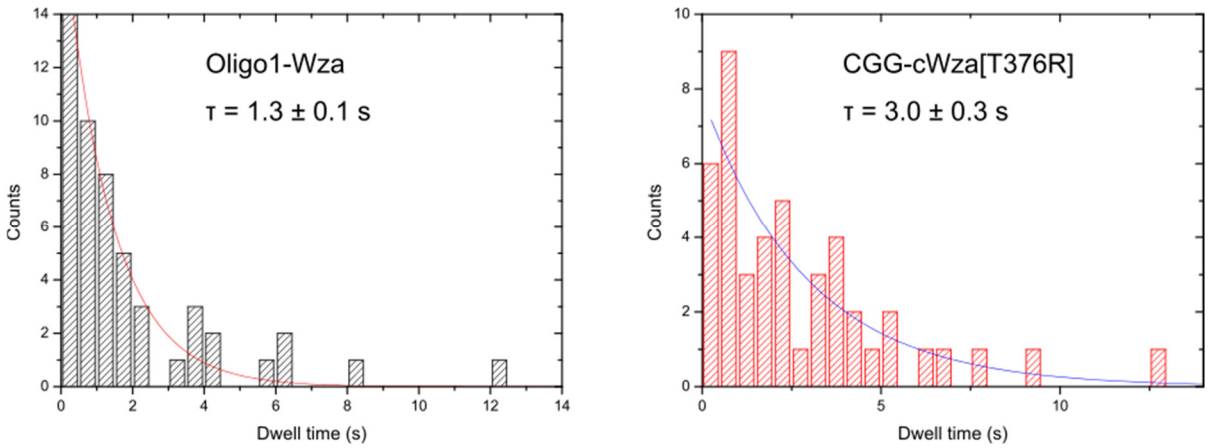


**Figure S13**. Lifetime of pores formed from free oligo1-Wza conjugates (-150 mV) and from free Wza peptides (+150 mV).

## *Scaffolded Wza peptides*

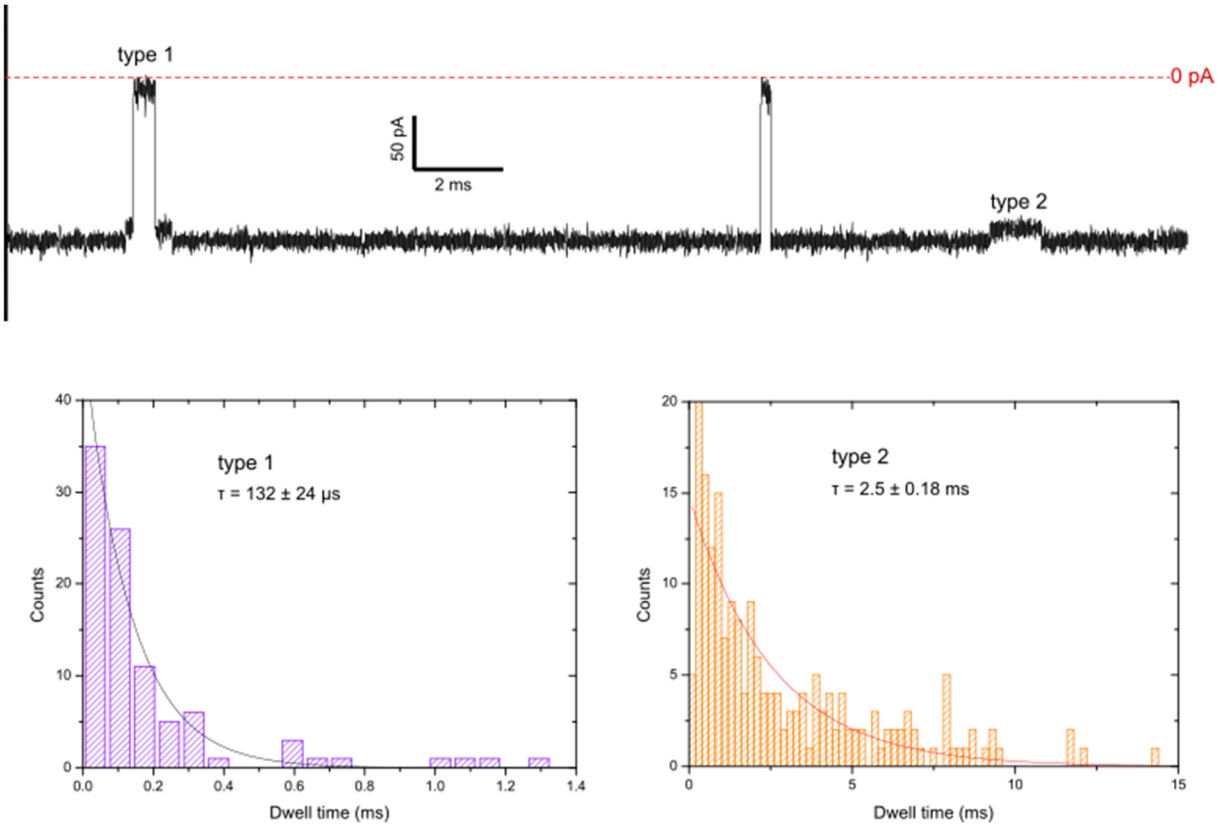


**Figure S14**. Top: segment of electrical recording from H-state of a scaffolded Wza octamer sampled at -100 mV and 50 kHz (filtered at 10 kHz), showing two types of subconductance: transient pore closing (type 1) and an open-pore subconductance (type 2). These two types of subconductance are observed in all scaffolded H-state Wza nanopores. Bottom: dwell time analysis of transient pore closing (type 1) and an open-pore subconductance state (type 2).

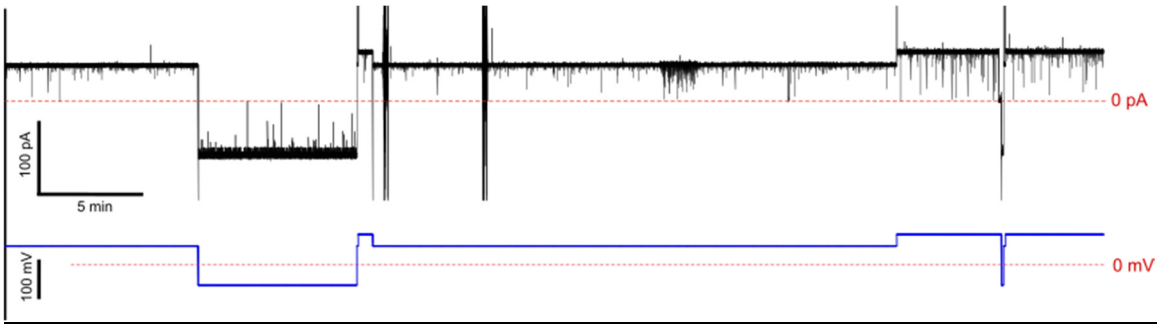


**Figure S15**. Prolonged recording of a pore from scaffolded Wza peptides in H-state (1 h total).

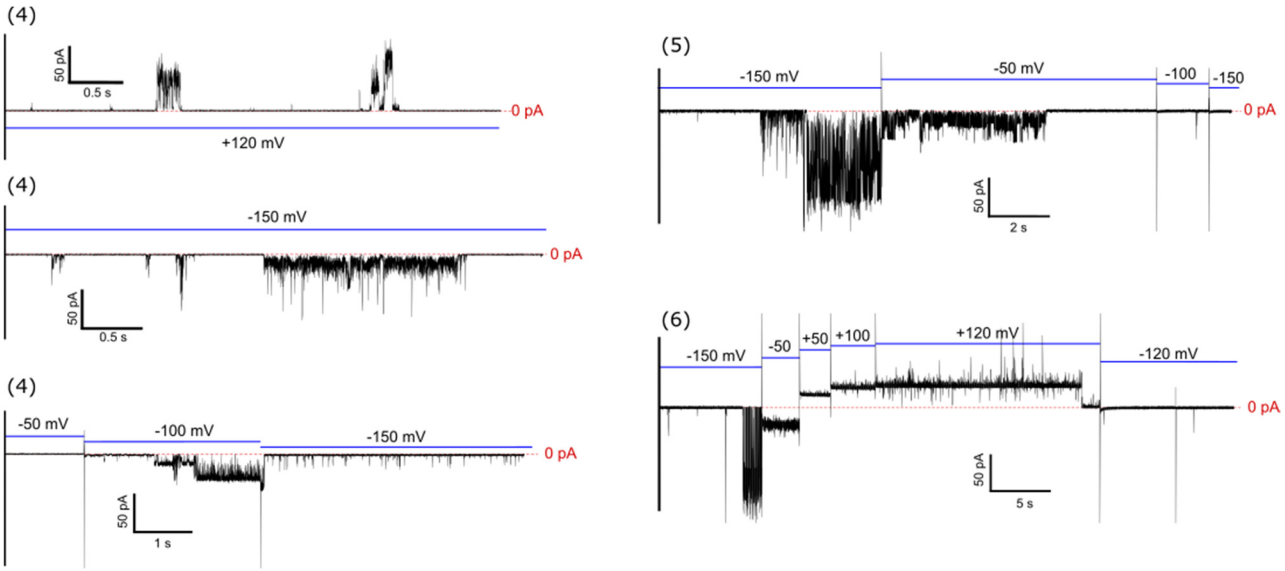


**Figure S16**. Electrical recordings of the insertion of unstable pores from scaffolds with fewer than 8 Wza peptides. The number of scaffolded Wza peptides is indicated by the numbers above each trace. The potential applied initially was +120 mV (top trace), and -150 mV (all other traces). The current signals were filtered at 2 kHz.

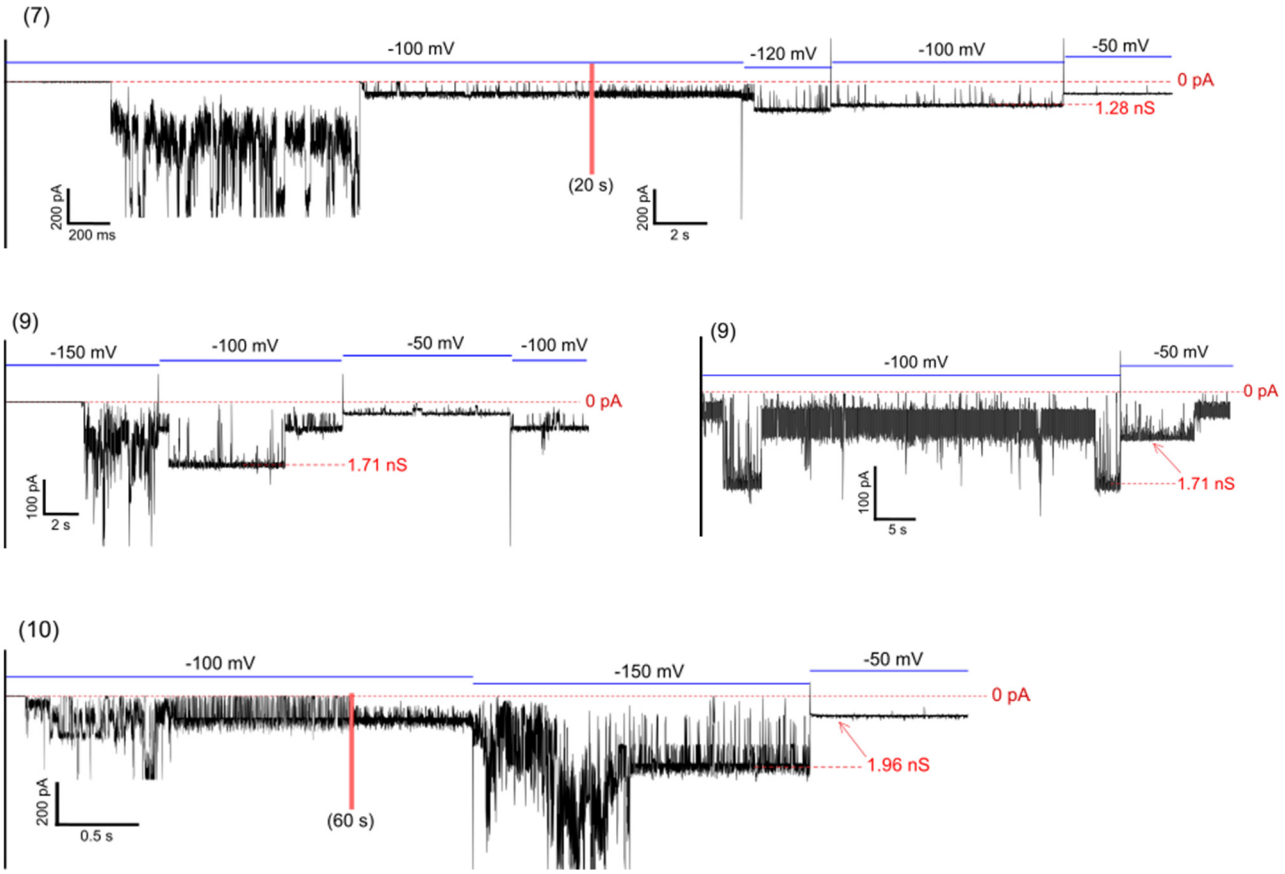


**Figure S17**. Electrical recordings displaying the insertion of pores with smaller or larger conductances than the 1.46 ± 0.06 usually observed for octamers. Top: a scaffold with 7 peptides, middle: a scaffold with 9 peptides, bottom: a scaffold with 10 peptides. In all cases, these pores are lost or return to an L-state within minutes. The current signals were filtered at 2 kHz.

## *Oligo-PEG binding to scaffolds*

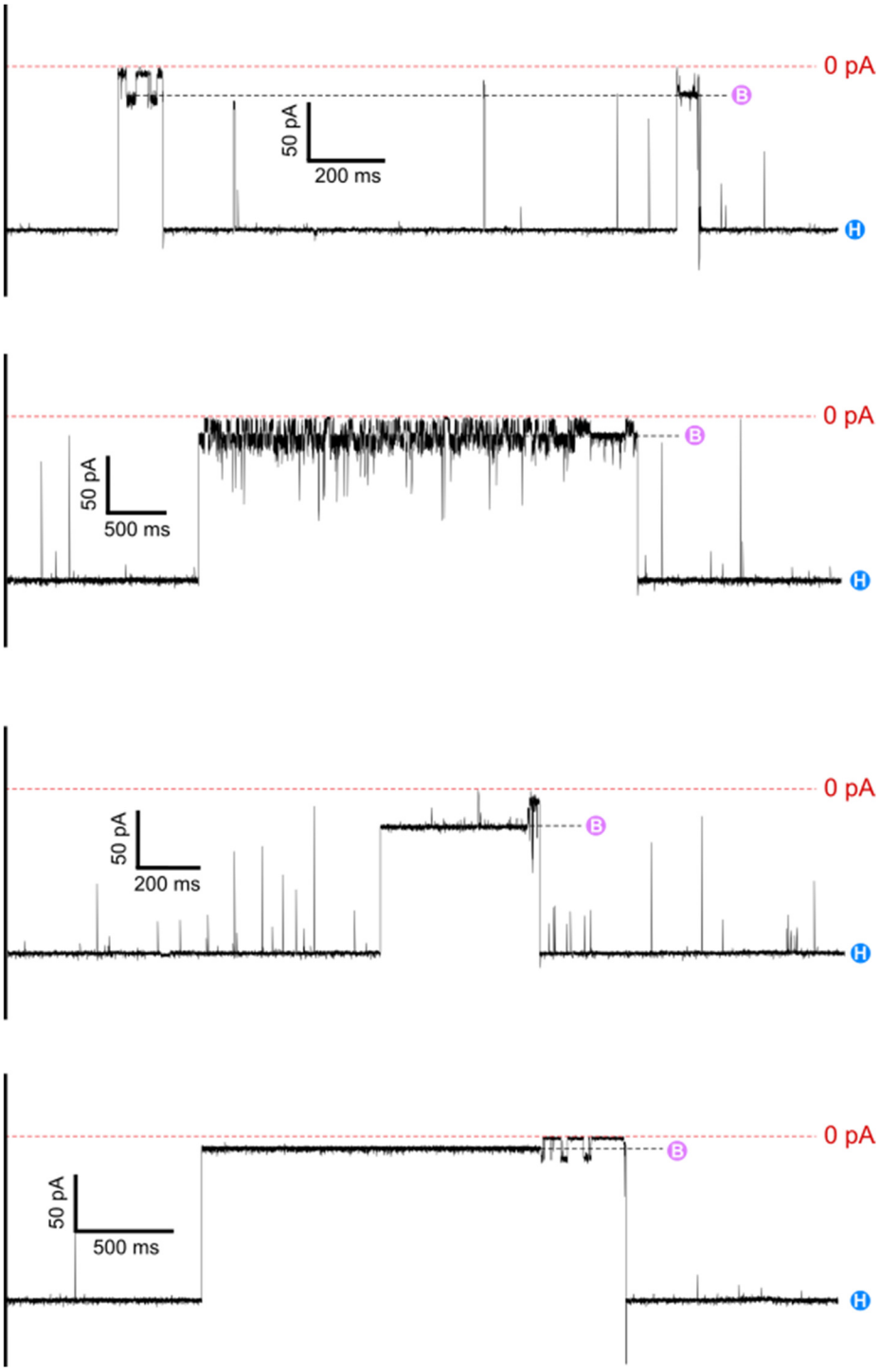


**Figure S18**. Electrical recordings showing reversible oligo-PEG binding (B) at -100 mV. In some cases, the conductance in the bound state fluctuates between two or more levels. The average current during a blockade (see for example the second trace) was used to calculate the residual current.

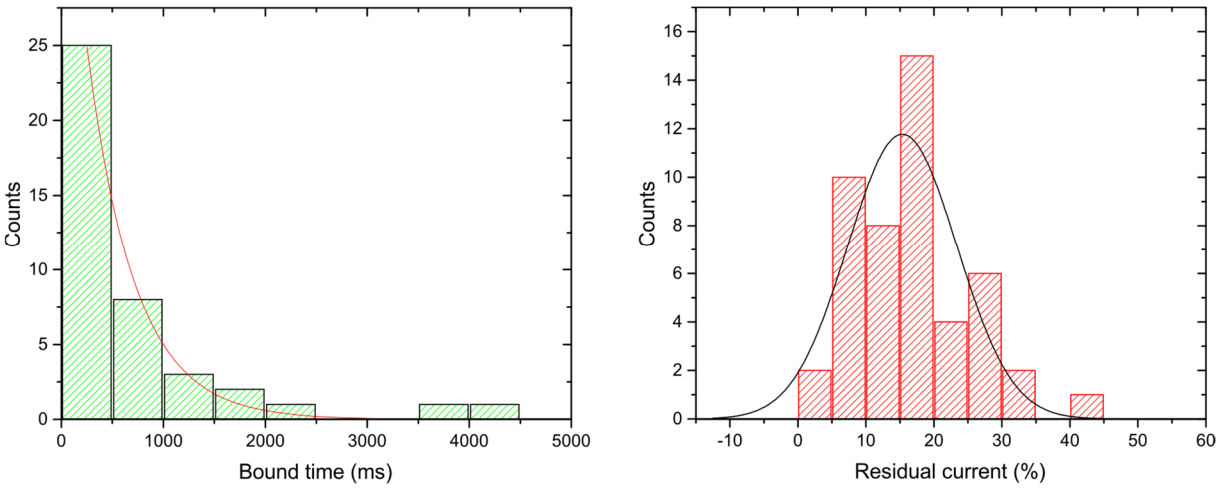


**Figure S19**. Lifetimes of states with oligo-PEG bound at -100 mV and event histogram of the residual current during blockades.

**Table S3**. Oligo-PEG binding characteristics.

| # oligo length | # events | V (mV) | Bound time (ms) | Residual current (%) |
|---|---|---|---|---|
| 8 | 53 | -100 | 466 ± 14 | 15.3 ± 1.2 |
| 19 | 2 experiments (irreversible binding) | -100 | Bound state observed for 5 and 12 min, resp., followed by bilayer disruption. | 11.4 ± 2.0<br>24.2 ± 1.7<br>(average of trace) |

## *Scaffolded C-terminal Wza peptides*

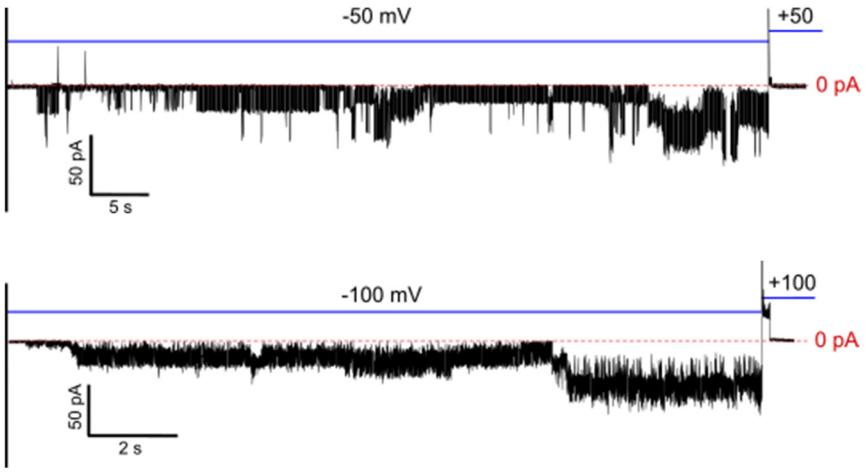


**Figure S20**. Electrical recordings of pores formed by Wza peptides scaffolded through their C termini. Eight peptides were attached to the scaffold. The current signals were filtered at 2 kHz.

# Supplementary References


1. Šulc, P., Romano, F., Ouldridge, T. E., Rovigatti, L., Doye, J. P. K. & Louis, A. A. Sequence-dependent thermodynamics of a coarse-grained DNA model. *J. Chem. Phys.* **137**, 135101 (2012).

2. Snodin, B. E. K., Randisi, F., Mosayebi, M., Šulc, P., Schreck, J. S., Romano, F.*, et al.* Introducing improved structural properties and salt dependence into a coarse-grained model of DNA. *J. Chem. Phys.* **142**, 234901 (2015).

3. Humphrey, W., Dalke, A. & Schulten, K. VMD: Visual molecular dynamics. *J. Mol. Graph.* **14**, 33-38 (1996).

4. Pettersen, E. F., Goddard, T. D., Huang, C. C., Couch, G. S., Greenblatt, D. M., Meng, E. C.*, et al.* UCSF Chimera—A visualization system for exploratory research and analysis. *J. Comp. Chem.* **25**, 1605-1612 (2004).

5. Rovigatti, L. Utility to convert coarse-graind representation into all-atom representation.[posted 15-08-2016]; Available from: https://sourceforge.net/p/oxdna/discussion/features/thread/1fcbb235/#121c

6. Sobott, F., Hernández, H., McCammon, M. G., Tito, M. A. & Robinson, C. V. A Tandem Mass Spectrometer for Improved Transmission and Analysis of Large Macromolecular Assemblies. *Anal. Chem.* **74**, 1402-1407 (2002).

7. Liko, I., Degiacomi, M. T., Mohammed, S., Yoshikawa, S., Schmidt, C. & Robinson, C. V. Dimer interface of bovine cytochrome c oxidase is influenced by local posttranslational modifications and lipid binding. *Proc. Natl Acad. Sci. USA* **113**, 8230-8235 (2016).

8. Hernandez, H. & Robinson, C. V. Determining the stoichiometry and interactions of macromolecular assemblies from mass spectrometry. *Nature Protoc.* **2**, 715-726 (2007).

9. Evans, G. W., Hohlbein, J., Craggs, T., Aigrain, L. & Kapanidis, A. N. Real-time single-molecule studies of the motions of DNA polymerase fingers illuminate DNA synthesis mechanisms. *Nucleic Acids Research* **43**, 5998-6008 (2015).

10. Gordon, M. P., Ha, T. & Selvin, P. R. Single-molecule high-resolution imaging with photobleaching. *Proc. Natl Acad. Sci. USA* **101**, 6462-6465 (2004).

11. Dave, R., Terry, D. S., Munro, J. B. & Blanchard, S. C. Mitigating Unwanted Photophysical Processes for Improved Single-Molecule Fluorescence Imaging. *Biophys. J.* **96**, 2371-2381 (2009).